DOI: 10.1109/IMS37964.2023.10187973

Characterization of a D-Band Electric-Inductive-Capacitive Metamaterial-Based Transmission Line Phase Shifter

***Abstract*— This paper presents the design of a phase shifter in the D-band, made by transmission lines loaded with electric-inductive-capacitive metamaterial resonators. The proposed design features a highly linear phase response and relatively low losses. Over a distance of about 1 mm, we achieved a 60°-100° phase shift with respect to the corresponding unloaded transmission line, which corresponds to a dimension reduction of the 45-49%. The device is realized in 130 nm SiGe BiCMOS technology, where active switching elements could be easily integrated to provide fast reconfigurability. The average insertion loss achieved in the operation band is 2.2 dB and reaches a maximum of 2.8 dB at 170 GHz. A 3D full-wave model is also reported in the paper: simulations allow good matching with the experiments, with relative error less than 7%.**

***Keywords*— metamaterial, phase-shifters, mm-wave.**

I. Introduction

The need for reconfigurable antenna arrays is a key point for the next mobile generation [1], especially in the range of mm-wave. To achieve beam-forming at such frequencies, tunable phase shifting components must be provided. Although vast literature on active phase shifter (PS) at mm-frequencies is present [2]–[5], such devices often present non-linear behavior and high losses. This represents an issue when dealing with high power or wide-band applications. It is therefore preferable to adopt passive solutions as suggested in [6]–[9]. The advantages of using metamaterial devices are the higher linearity, the low power consumption and the bidirectional response, granting better performances in both transmitting and receiving systems. In this paper, we present the characterization of a metamaterial-based transmission line phase shifter at 140 GHz, using Electric-Inductive-Capacitive (ELC) metamaterial cells [10]. The device has been designed and fabricated in 0.13-μm SiGe BiCMOS (SG13) technology. Consequently, a full-wave electromagnetic model has been implemented in order to provide an effective tool to characterize the behavior of the phase shifter. In Section III we compare our model with the measurement and present an analysis of the structure varying the number of metacells and the dimension of the inductive ring.

II. Device model and fabrication

The device, as shown in Fig 1, is composed by a microstrip line above an array of metacell couples. In this work we opted for an ELC metamaterial resonator, as shown in Fig.2. As reported in [10], the cell present an interdigitated capacitor to reduce the size of the resonator. The cell is designed to resonate outside the interest band so that the phase-shift is obtained without the huge losses due to resonances. The parameter d, related to the inductive element, is considered as a degree of freedom and in this study we considered values of 4 μm ,10 μm and 16 μm.

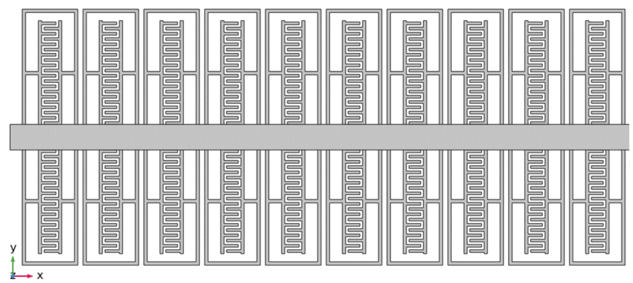

Fig. 1. Top view of the model geometry. The microstrip is positioned in a layer above the metacell array. Substrate is hidden for clarity.

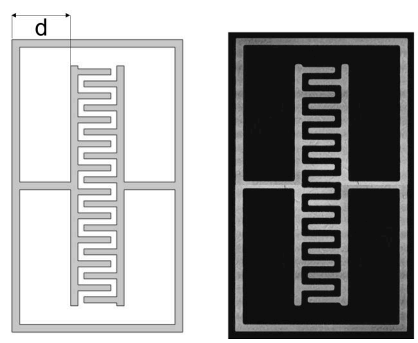

Fig. 2. Schematic representation of the metacell. Geometry model (right) laser microscope image (left)

The phase shifter is realized in state-of-the-art 0.13-μm SiGe BiCMOS (SG13) as shown in Fig. 3. Multiple lines with different cell numbers and sizes are fabricate and measured as it will be reported in Secion III.

The complete model of the microstrip with the metacell array in Fig. 1 is implemented using the software COMSOL Multiphysics and it presents the parameter listed in Table 1.

III. Results

To avoid defective transmission lines or production flaws in some sections of the wafer, multiple structures have

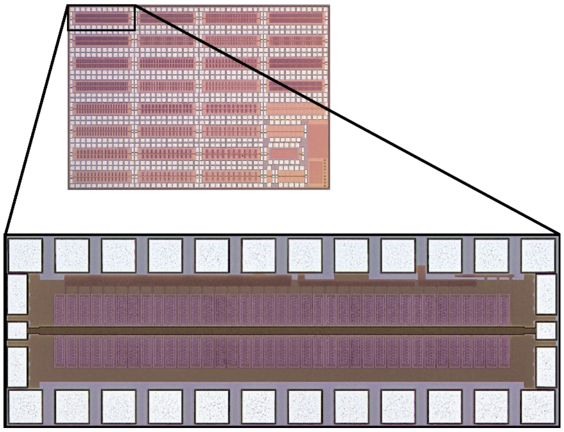

Fig. 3. Wafer section with multiple phase-shifter for the measurement and calibration seen by an optical microscope. (zoom) Single phase-shifter geometry with length l = 1 mm

Table 1. Parameter list used in the model

Parameter	Value
Line length (l)	1.00 mm
Line width (w)	16.0 μm
Cell thickness	2.00 μm
Cell-Line distance	2.80 μm
Cell-Ground distance	4.97 μm
Cell-Cell distance	0.00 μm
Dielectric thickness	9.77 μm

been realized on the wafer and multiple measurements have been performed. Fig. 4 shows the S-parameters obtained operating a Multi-Thru-Reflect-Line (MTRL) calibration on the measurement. It is possible to see how the curves do not sensibly change from a section to another. As shown in Fig. 4, the average insertion loss in the full band is 2.2 dB and it reaches a maximum of 2.8 dB at 170 GHz.

We now consider a microstrip with metacells with d = 10 μm, however similar results are obtained from structures with different d values. As shown in Fig. 5 and 6, the simulation results match the measurement data in the amplitude and the phase, proving that the model is a good approximation of the real structure and the MTRL calibration is effective. As expected, the phase, shown in Fig. 6, is highly linear in frequency.

Fig. 7 represents the phase shift of the device considering different cell dimensions given a fixed number of 15 metacells under the line. At 140 GHz the phase shift of the metamaterial line is 80° higher compared to the normal microstrip. The phase remains highly linear with the exception of the line with metacells with d = 16 μm. In this case, the curve presents a maximum at around 163 GHz due to the increased inductive element that reduces the resonance frequency of the metacells.

Fig. 8 represents the phase shift of the device with d fixed and variable number of cells.

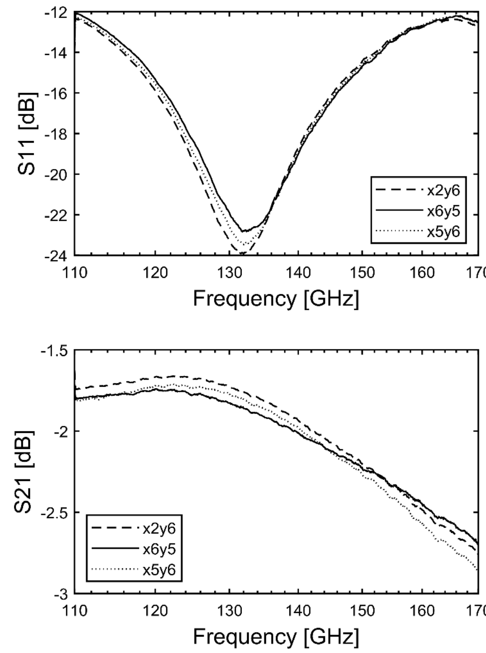

Fig. 4. Measured S-parameters. Different curves belong to different areas of the Wafer, with sections addressed with x and y coordinates in a grid

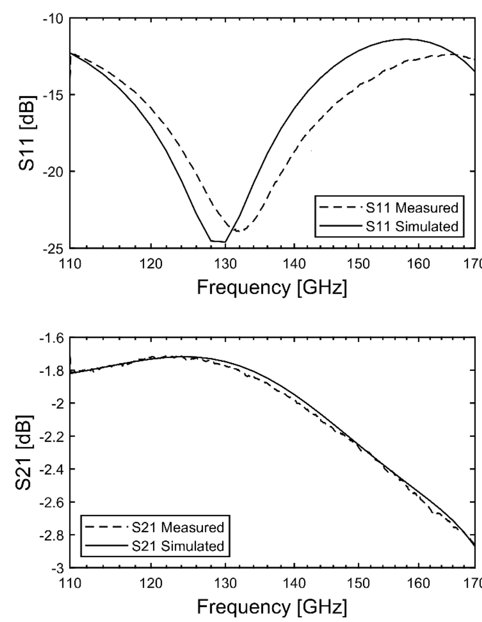

Fig. 5. Comparison between the magnitude of S_{11} (top) and S_{21} (bottom) in measurements and model simulations.

The phase shift increase with the number of cells, however with more than 20 metacells the phase shift seems to saturate. This is due to the interaction between near cells. Since the length of the line is fixed, increasing the number of cells means a reduction of the distance between the adjacent ones. It is, therefore, reasonable that each cell couples with part of the fields radiated from the near ones, reducing their effect on the microstrip. Compared to the microstrip without metacells in the 110-170 GHz band, we achieved a 60°-100° phase shift

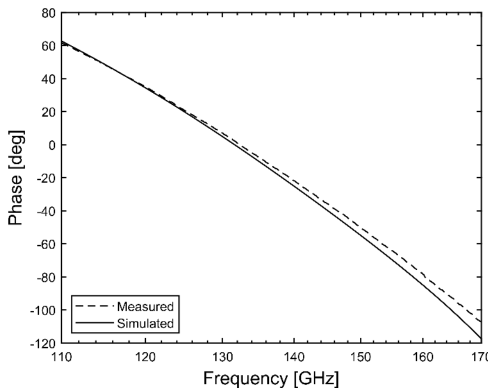

Fig. 6. Comparison of the phase shift between measurements and model simulaions.

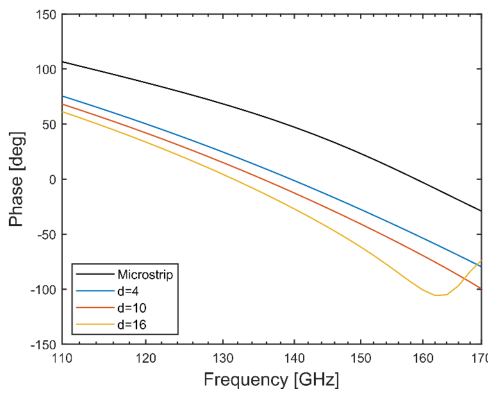

Fig. 7. Comparison of the phase shift with different dimension d of the metacells. The number of cells is fixed to 15.

which corresponds to a dimension reduction of the 45-49%.

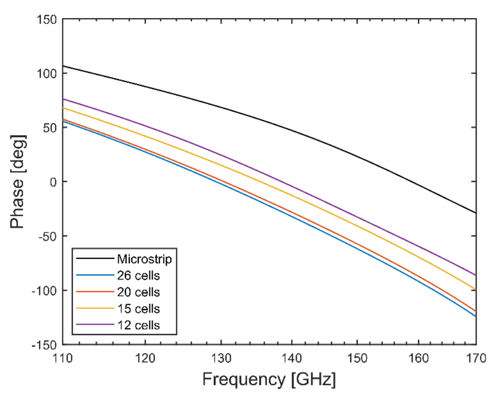

Fig. 8. Comparison of the phase shift with different number of cells. The dimension of the metacells is d = 10 μm.

IV. Conclusion

In this paper we presented a phase shifter based on a ELC metacell microstrip line, working in D-band. Such device achieved a 60° - 100° quasi-linear phase shift in the 110-170 GHz band. This shift corresponds to a dimension reduction of the 45-49%. The average insertion loss in the full band is 2.2 dB and it reaches the maximum value of 2.8 dB at 170 GHz. The presented model matches experiments with good approximation and presents a maximum relative error, compared to the measurements, of 7%. Thanks to such model, in future works, it will be possible to test different topologies and investigate the introduction of active elements in order to tune the metacell resonance and, thus, the phase shift.

Acknowledgment

References

[1] A. L. Swindlehurst, E. Ayanoglu, P. Heydari, and F. Capolino, "Millimeter-wave massive mimo: the next wireless revolution?" *IEEE Communications Magazine*, vol. 52, no. 9, pp. 56–62, 2014.

[2] Y. Xiong, X. Zeng, and J. Li, "A frequency-reconfigurable cmos active phase shifter for 5g mm-wave applications," *IEEE Transactions on Circuits and Systems II: Express Briefs*, vol. 67, no. 10, pp. 1824–1828, 2020.

[3] D. Pepe and D. Zito, "Two mm-wave vector modulator active phase shifters with novel iq generator in 28 nm fdsoi cmos," *IEEE Journal of Solid-State Circuits*, vol. 52, no. 2, pp. 344–356, 2017.

[4] P. Song and H. Hashemi, "Wideband mm-wave phase shifters based on constant-impedance tunable transmission lines," in *2016 IEEE MTT-S International Microwave Symposium (IMS)*, 2016, pp. 1–4.

[5] P. B. Vadivelu, P. Sen, S. Sarkar, D. Dawn, S. Pinel, and J. Laskar, "Integrated cmos mm-wave phase shifters for single chip portable radar," in *2009 IEEE MTT-S International Microwave Symposium Digest*, 2009, pp. 565–568.

[6] Y. Tousi and A. Valdes-Garcia, "A ka-band digitally-controlled phase shifter with sub-degree phase precision," in *2016 IEEE Radio Frequency Integrated Circuits Symposium (RFIC)*, 2016, pp. 356–359.

[7] C.-Y. Kim, D.-W. Kang, and G. M. Rebeiz, "A 44–46-ghz 16-element sige bicmos high-linearity transmit/receive phased array," *IEEE Transactions on Microwave Theory and Techniques*, vol. 60, no. 3, pp. 730–742, 2012.

[8] M.-D. Tsai and A. Natarajan, "60ghz passive and active rf-path phase shifters in silicon," in *2009 IEEE Radio Frequency Integrated Circuits Symposium*, 2009, pp. 223–226.

[9] H. Krishnaswamy, A. Valdes-Garcia, and J.-W. Lai, "A silicon-based, all-passive, 60 ghz, 4-element, phased-array beamformer featuring a differential, reflection-type phase shifter," in *2010 IEEE International Symposium on Phased Array Systems and Technology*, 2010, pp. 225–232.

[10] W. Withayachumnankul, C. Fumeaux, and D. Abbott, "Compact electric-lc resonators for metamaterials," *Opt. Express*, vol. 18, no. 25, pp. 25 912–25 921, Dec 2010. [Online]. Available: https://opg.optica.org/oe/abstract.cfm?URI=oe-18-25-25912